

Optimized pilot distribution to track the phase noise in DFT-s-OFDM for sub-THz systems

J.-C. Sibel, V. Corlay, and A. Bechihi

Mitsubishi Electric R&D Centre Europe

Rennes, France

Email: {j.sibel, v.corlay, a.bechihi}@fr.mercede.mee.com

Abstract—In this paper, we focus on the selection of a pilot pattern to track the phase noise in high frequency bands in a DFT-s-OFDM chain. By considering the Wiener filter at the receiver side to perform the tracking, we use the inner cost function of the said filter as the cost function for the pilot selection. To obtain this cost function, the phase noise autocorrelation is required. Therefore, we introduce a new mathematical approximation of the autocorrelation function of the practical 3GPP phase noise model. At first, this leads to an analytical expression of the Wiener filter coefficients. Then, the said coefficients allow us to obtain an analytical expression of the cost function. Thus, by means of this result, we are able to provide a pilot pattern that jointly satisfies a constraint on the pilot overhead and a constraint on the minimum performance of the Wiener filter.

Index Terms—Sub-THz bands, phase noise, Wiener filter.

INTRODUCTION

3GPP NR specifications provide the 5G technology to take benefit of high frequency ranges, namely mmWaves, until 71GHz [1]. It is expected that sub-THz frequencies and beyond will be used for the 6G technology [2]. This opens the room for greater bandwidths, higher data rates, etc. However, working with such high frequency values is not straightforward because of the limited capability of hardware materials. Among others, the phase noise is a phenomenon that stems from this limitations and that induces an increasing and negative impact on signals as the carrier frequency increases. Even though some futuristic components might be developed to cancel this limitation, the 3GPP specifications provide dedicated pilots called Phase Tracking Reference Signals (PT-RS) that enable to estimate and track the phase noise to work with good communication performance [3].

The PT-RS can be distributed in several manners depending on the waveform, the bandwidth, the subcarrier spacing, the Modulation and Coding Scheme (MCS), etc. In this paper, we consider an Orthogonal Frequency-Division Multiplexing (OFDM) chain with a Discrete Fourier Transform (DFT) precoding, simply called DFT-s-OFDM [4]. For this case, the PT-RS are inserted in the time domain before the DFT precoding in equally spaced groups. During the phase of specifications, the decisions on the values of group sizes and group spacings were made based on numerical evaluations of the whole DFT-s-OFDM chain from several companies [5]. The drawback in this approach is that results also depends, at least, on the MCS that is out of the tracking algorithm. It

would be more relevant to select the PT-RS pattern based on the performance of the tracking algorithm only.

In this paper, we focus on the Wiener filter [6] to track the phase noise which is a usual scheme used in wireless communications. The filter coefficients are obtained by minimizing a cost function J that is determined by the autocorrelation function of the phase noise. The analytical expression is not available for the practical model of 3GPP [7] usually used in the literature. To overcome this difficulty, we propose an analytical approximation of the said autocorrelation function based on its graphical shape which helps obtain an analytical expression of J . Out of this effort, we are given the possibility to analyze and predict the behavior of J as a function of the simulation parameters, e.g., the carrier frequency and the PT-RS spacing. Indeed, including one constraint related to an arbitrary maximum value of J and one constraint related to a maximum overhead for the sake of the spectral efficiency, we are able to extract the PT-RS spacing that minimizes J , i.e., that offers the best performance of the Wiener filter. As in the 3GPP specifications, we consider the PT-RS to be equally spaced and we simplify the study by assuming that the PT-RS groups are of size one.

Contributions - We provide an analytical model of the autocorrelation function for the 3GPP phase noise model. Based on this, we provide the analytical expression of the Wiener filter coefficients. From this, we derive an analytical form of the cost function J as a function of the PT-RS spacing. We show that through numerical evaluations a linear approximation of J is equivalent. We finally show how to select the PT-RS spacing that satisfies a constraint on J as well as a constraint on the PT-RS overhead.

The paper is structured as follows. Section I presents the considered communication chain and describes our approximation of the 3GPP phase noise model. Then, Section II exposes the Wiener filter computation with the derivation of the filter coefficients based on our approximation model. Section III presents the associated derivation of the cost function of the Wiener filter using the previously computed filter coefficients and a analysis of its behavior. Finally, Section IV describes the method for obtaining the PT-RS spacing that fulfills a maximum cost constraint and a maximum overhead constraint with an application example.

I. PHASE NOISE IN DFT-S-OFDM

This section presents the DFT-s-OFDM chain and an analytical approximation of the 3GPP phase noise model.

A. Communication chain

We consider a single DFT-s-OFDM symbol $\underline{x} = [x_1 \dots x_N]$ of length N where x_n is a constellation symbol (QAM, PSK). The phase noise $\underline{\alpha} = [\alpha_1 \dots \alpha_N]$ affects the signal, where $\alpha_n = e^{i\phi_n}$. Then, an AWGN $\underline{z} = [z_1 \dots z_N]$ also alters the signal, where $z_n \sim \mathcal{CN}(0, \sigma_z^2)$. Hence, we get the received signal $\underline{y} = [y_1 \dots y_N]$ with:

$$y_n = \alpha_n x_n + z_n. \quad (1)$$

We allocate N_P pilots whose indexes in the symbol \underline{x} are p_1, \dots, p_{N_P} . We assume the pilots to be uniformly distributed such that the position difference between any two consecutive pilots p_j, p_{j+1} is $\Delta = |p_{j+1} - p_j|$. Accordingly, for $1 \leq j \leq N_P$, the j^{th} pilot index is:

$$p_j = p_1 + (j - 1)\Delta. \quad (2)$$

On each pilot index j , provided that $|x_{p_j}|^2 = 1$, we assume a least-square (LS) estimate of the phase noise:

$$\tilde{\alpha}_{p_j} \stackrel{\text{def}}{=} y_{p_j} \bar{x}_{p_j}, \quad (3)$$

where \bar{x}_{p_j} stems for the complex conjugate of x_{p_j} . This amounts to:

$$\tilde{\alpha}_{p_j} = \alpha_{p_j} + \tilde{z}_{p_j}, \quad (4)$$

where $\tilde{z}_{p_j} = z_{p_j} \bar{x}_{p_j}$ follows the same law as z_{p_j} . The performance of any phase noise tracking process become relevant when working at high Signal-to-Noise Ratio (SNR) values, see the evaluation results in [8]. Consequently, we assume in the rest of the paper that the SNR is infinite such that $\sigma_z = 0$ meaning that:

$$y_n = \alpha_n x_n. \quad (5)$$

B. Phase noise exponential model

We consider the phase noise model from the 3GPP specifications [7, 4.2.3.1] that scales with the carrier frequency F_c .

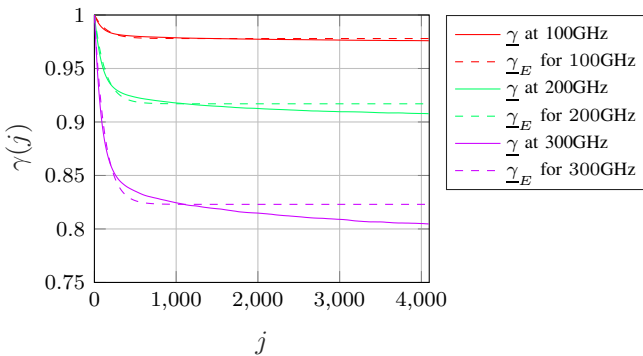


Fig. 1. Empirical autocorrelation of the 3GPP model in solid lines, exponential approximation $\mathcal{E}_N(a, b)$ in dashed lines.

By plotting the subsequent empirical autocorrelation function $\gamma(j) = \mathbb{E}[\alpha_n \alpha_{n-j}^*]$ of the generated $\underline{\alpha}$, see Fig. 1, we observe a bimodal behavior. For low values of j , $\gamma(j)$ follows an exponential decrease like $e^{-a|j|}$ with $a \in \mathbb{R}_+$. For middle/large values of j , $\gamma(j)$ follows a linear decrease. The slope is low enough to consider a simple floor limit $\gamma(j) \approx b$ with $b \in \mathbb{R}$. From these observations, then, we propose the *exponential model* $\mathcal{E}_N(a, b)$:

$$\gamma_E(j) \stackrel{\text{def}}{=} \frac{e^{-a|j|} + \frac{b}{1-b}}{1 + \frac{b}{1-b}}. \quad (6)$$

The couple (a, b) is found by minimizing the mean square error between $\underline{\gamma}$ and $\underline{\gamma}_E$. Fig. 1 exhibits $\underline{\gamma}$ and $\underline{\gamma}_E$ with the said parameters for several values of F_c . The evolution of a, b as functions of F_c are displayed in Fig. 2(a) and Fig. 2(b). We observe that a does not change a lot with F_c compared to the change of b with F_c . Therefore, an increase in the carrier frequency mainly involves a negative offset in the autocorrelation function which corresponds to a decrease in the correlation between the phase noise samples. This is consistent with the hypothesis of an uncorrelated phase noise model for very high frequencies proposed in [9].

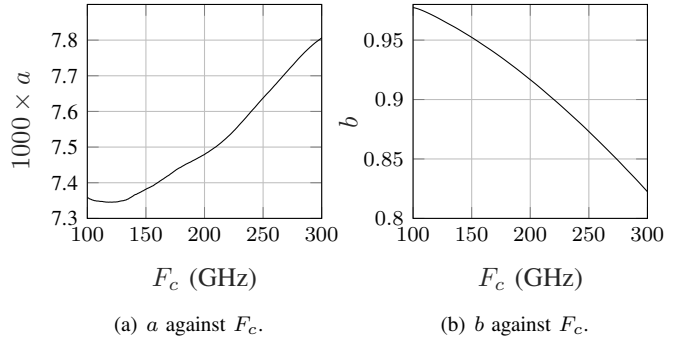


Fig. 2. Optimal parameters of $\mathcal{E}_N(a, b)$.

II. WIENER FILTER

This section presents the Wiener filter for tracking the phase noise when using the exponential model of the phase noise autocorrelation. The series of calculations is a tedious process that is not of a strong interest for the current paper. Therefore, here after, we only provide some clues and main results for mathematical derivations. The interested reader can refer to [10] to get the whole demonstration.

A. Basics

From [6], the Wiener filter provides an estimate of α_n :

$$\hat{\alpha}_n = \underline{w}_n^T \tilde{\alpha}_p, \quad (7)$$

where $\underline{w}_n \stackrel{\text{def}}{=} [w_{n,1} \dots w_{n,N_P}]$ are the filter coefficients and $\tilde{\alpha}_p \stackrel{\text{def}}{=} [\tilde{\alpha}_{p_1} \dots \tilde{\alpha}_{p_{N_P}}]$ are the LS estimates on the pilot positions. The filter error is defined as $e_n \stackrel{\text{def}}{=} \alpha_n - \hat{\alpha}_n$ and the associated cost function is defined as:

$$J_n \stackrel{\text{def}}{=} \mathbb{E}[|e_n|^2]. \quad (8)$$

The optimal filter coefficients \hat{w}_n are obtained by minimizing J_n through a derivative calculation. It can be shown [6] that this amounts to:

$$\hat{w}_n = R^{-1} \underline{\gamma}_n, \quad (9)$$

where R is the *pilot autocorrelation matrix* of size $N_p \times N_p$ such that $R_{i,j} = \gamma(p_j - p_i)$ and $\underline{\gamma}_n$ is the *autocorrelation vector* of size $N_p \times 1$ between a phase noise sample α_n (position n) and all the pilot positions p_1, \dots, p_{N_p} , such that the j^{th} coordinate of $\underline{\gamma}_n$ is $\gamma(n - p_j)$. The autocorrelation function is then necessary to derive the analytical form of the Wiener filter coefficients.

B. Autocorrelation vector

We use the exponential model $\mathcal{E}_N(a, b)$ to replace γ in (9). This makes the correlation vector become:

$$\underline{\gamma}_n = \frac{1}{1+c} \left(\begin{bmatrix} e^{-a|n-p_1|} \\ e^{-a|n-p_2|} \\ \vdots \\ e^{-a|n-p_{N_p}|} \end{bmatrix} + c \begin{bmatrix} 1 \\ 1 \\ \vdots \\ 1 \end{bmatrix} \right). \quad (10)$$

with $c \stackrel{\text{def}}{=} \frac{b}{1-b}$. Given (2), it is possible to remove the dependence in the pilot position p_j which will be convenient in the rest of the paper. Defining $\lambda \stackrel{\text{def}}{=} e^{-a\Delta}$, it comes that:

$$e^{-a|n-p_j|} = \begin{cases} e^{-a(p_1-n)} \lambda^{j-1} & n \leq p_j \\ e^{-a(n-p_1)} \lambda^{1-j} & \text{otherwise} \end{cases}. \quad (11)$$

C. Pilot autocorrelation matrix

We can show that the autocorrelation matrix R is the following sum:

$$R = \frac{c}{1+c} \left(\frac{1}{c} A_\lambda + J_{N_p} \right), \quad (12)$$

with:

$$A_\lambda \stackrel{\text{def}}{=} \begin{bmatrix} 1 & \lambda & \dots & \lambda^{N_p-1} \\ \lambda & 1 & \dots & \lambda^{N_p-2} \\ \vdots & \vdots & \ddots & \vdots \\ \lambda^{N_p-1} & \lambda^{N_p-2} & \dots & 1 \end{bmatrix}, \quad (13)$$

and:

$$J_{N_p} \stackrel{\text{def}}{=} \begin{bmatrix} 1 & 1 & \dots & 1 \\ 1 & 1 & \dots & 1 \\ \vdots & \vdots & \ddots & \vdots \\ 1 & 1 & \dots & 1 \end{bmatrix}. \quad (14)$$

Defining the all-ones column vector \underline{u} of length N_p , it comes that $J_{N_p} = \underline{u}\underline{u}^T$. From (12), we can say that:

$$R^{-1} = \frac{1+c}{c} \left(\frac{1}{c} A_\lambda + J_{N_p} \right)^{-1}, \quad (15)$$

Now, we make use of the Sherman-Morrison formula from *weblink* that leads to:

$$R^{-1} = (1+c) \left(A_\lambda^{-1} - c \frac{A_\lambda^{-1} J_{N_p} A_\lambda^{-1}}{1 + c \underline{u}^T A_\lambda^{-1} \underline{u}} \right). \quad (16)$$

According to [11] we can invert invert A_λ s.t.:

$$A_\lambda^{-1} = \frac{X_\lambda}{1-\lambda^2}, \quad (17)$$

with:

$$X_\lambda \stackrel{\text{def}}{=} \begin{bmatrix} 1 & -\lambda & 0 & \dots & \dots & \dots & 0 \\ -\lambda & 1+\lambda^2 & -\lambda & 0 & & & \vdots \\ 0 & -\lambda & 1+\lambda^2 & -\lambda & 0 & & \vdots \\ \vdots & \ddots & \ddots & \ddots & \ddots & \ddots & \vdots \\ \vdots & & 0 & -\lambda & 1+\lambda^2 & -\lambda & 0 \\ \vdots & & & 0 & -\lambda & 1+\lambda^2 & -\lambda \\ 0 & \dots & \dots & \dots & 0 & -\lambda & 1 \end{bmatrix}. \quad (18)$$

Now, we compute (16) step-by-step. First of all, we can show that:

$$A_\lambda^{-1} J_{N_p} = \frac{1}{1+\lambda} \begin{bmatrix} 1 & \dots & 1 \\ 1-\lambda & \dots & 1-\lambda \\ \vdots & & \vdots \\ 1-\lambda & \dots & 1-\lambda \\ 1 & \dots & 1 \end{bmatrix}. \quad (19)$$

This leads to the calculation of the numerator of the fraction in (16):

$$A_\lambda^{-1} J_{N_p} A_\lambda^{-1} = \frac{Y_\lambda}{(1+\lambda)^2}, \quad (20)$$

with:

$$Y_\lambda \stackrel{\text{def}}{=} \begin{bmatrix} 1 & 1-\lambda & \dots & 1-\lambda & 1 \\ 1-\lambda & (1-\lambda)^2 & \dots & (1-\lambda)^2 & 1-\lambda \\ \vdots & \vdots & & \vdots & \vdots \\ 1-\lambda & (1-\lambda)^2 & \dots & (1-\lambda)^2 & 1-\lambda \\ 1 & 1-\lambda & \dots & 1-\lambda & 1 \end{bmatrix}. \quad (21)$$

After that, we focus on the denominator of the fraction in (16). First, we compute:

$$A_\lambda^{-1} \underline{u} = \frac{1}{1+\lambda} \begin{bmatrix} 1 \\ 1-\lambda \\ \vdots \\ 1-\lambda \\ 1 \end{bmatrix}. \quad (22)$$

Then, it comes that:

$$\underline{u}^T A_\lambda^{-1} \underline{u} = \frac{2\lambda + (1-\lambda)N_p}{1+\lambda}. \quad (23)$$

Merging the result for the numerator and the denominator provides the following formula for the fraction:

$$c \frac{A_\lambda^{-1} J_{N_p} A_\lambda^{-1}}{1 + c \underline{u}^T A_\lambda^{-1} \underline{u}} = \frac{c Y_\lambda}{(1+\lambda)(1+\lambda+2\lambda c + (1-\lambda)cN_p)}. \quad (24)$$

Now, we deduce the equivalent form of R^{-1} in (16):

$$R^{-1} = \frac{1+c}{1+\lambda} \left(\frac{X_\lambda}{1-\lambda} - \frac{c Y_\lambda}{1+\lambda+2\lambda c + (1-\lambda)cN_p} \right). \quad (25)$$

D. Wiener filter coefficients

We inject (10) and (25) in (9) to obtain a closed form of the Wiener filter coefficients. To this end, we inject the expression of R^{-1} from the previous section which results in $\hat{w}_n = \hat{w}_n^{(X)} - \hat{w}_n^{(Y)}$ with:

$$\hat{w}_n^{(X)} \stackrel{\text{def}}{=} \frac{1+c}{(1+\lambda)(1-\lambda)} X_\lambda \gamma_n, \quad (26)$$

$$\hat{w}_n^{(Y)} \stackrel{\text{def}}{=} \frac{c(1+c)}{(1+\lambda)(1+\lambda+2\lambda c+(1-\lambda)cN_P)} Y_\lambda \gamma_n. \quad (27)$$

Firstly, in the formula of $\hat{w}_n^{(X)}$ we can show that:

$$(1+c)X_\lambda \gamma_n = \begin{pmatrix} c(1-\lambda) \begin{bmatrix} 1 \\ 1-\lambda \\ \vdots \\ 1-\lambda \\ 1 \end{bmatrix} \\ + \begin{bmatrix} e^{-a|n-p_1|} - \lambda e^{-a|n-p_2|} \\ (1+\lambda^2)e^{-a|n-p_2|} - \lambda(e^{-a|n-p_1|} + e^{-a|n-p_3|}) \\ \vdots \\ (1+\lambda^2)e^{-a|n-p_j|} - \lambda(e^{-a|n-p_{j-1}|} + e^{-a|n-p_{j+1}|}) \\ \vdots \\ (1+\lambda^2)e^{-a|n-p_{N_P-1}|} - \lambda(e^{-a|n-p_{N_P-2}|} + e^{-a|n-p_{N_P}|}) \\ e^{-a|n-p_{N_P}|} - \lambda e^{-a|n-p_{N_P-1}|} \end{bmatrix} \end{pmatrix}, \quad (28)$$

(28)

(29)

where the row with p_j is the j^{th} row of the matrix. Therefore:

$$\hat{w}_n^{(X)} = \frac{1}{1-\lambda^2} \begin{bmatrix} e^{-a|n-p_1|} - \lambda e^{-a|n-p_2|} \\ (1+\lambda^2)e^{-a|n-p_2|} - \lambda(e^{-a|n-p_1|} + e^{-a|n-p_3|}) \\ \vdots \\ (1+\lambda^2)e^{-a|n-p_j|} - \lambda(e^{-a|n-p_{j-1}|} + e^{-a|n-p_{j+1}|}) \\ \vdots \\ (1+\lambda^2)e^{-a|n-p_{N_P-1}|} - \lambda(e^{-a|n-p_{N_P-2}|} + e^{-a|n-p_{N_P}|}) \\ e^{-a|n-p_{N_P}|} - \lambda e^{-a|n-p_{N_P-1}|} \end{bmatrix} \times \begin{bmatrix} 1 \\ 1-\lambda \\ \vdots \\ 1-\lambda \\ 1 \end{bmatrix} + \frac{c}{1+\lambda} \begin{bmatrix} 1 \\ 1-\lambda \\ \vdots \\ 1-\lambda \\ 1 \end{bmatrix}. \quad (30)$$

Secondly, in the formula of $\hat{w}_n^{(Y)}$ it can be shown that:

$$(1+c)Y_\lambda \gamma_n = (\beta_n + \rho_\lambda) \begin{bmatrix} 1 \\ 1-\lambda \\ \vdots \\ 1-\lambda \\ 1 \end{bmatrix}, \quad (31)$$

with:

$$\beta_n \stackrel{\text{def}}{=} \sum_{j=1}^{N_P} e^{-a|n-p_j|} - \lambda \sum_{j=2}^{N_P-1} e^{-a|n-p_j|}, \quad (32)$$

$$\rho_\lambda \stackrel{\text{def}}{=} \lambda c(2 - N_P) + cN_P. \quad (33)$$

Therefore:

$$\hat{w}_n^{(Y)} = \frac{c(\beta_n + \rho_\lambda)}{(1+\lambda)(1+\lambda+\rho_\lambda)} \begin{bmatrix} 1 \\ 1-\lambda \\ \vdots \\ 1-\lambda \\ 1 \end{bmatrix}. \quad (34)$$

Now, using (30) and (34), we obtain \hat{w}_n :

$$\hat{w}_n = \frac{c(1+\lambda-\beta_n)}{(1+\lambda)(1+\lambda+\rho_\lambda)} \begin{bmatrix} 1 \\ 1-\lambda \\ \vdots \\ 1-\lambda \\ 1 \end{bmatrix} + \frac{1}{1-\lambda^2} \begin{bmatrix} e^{-a|n-p_1|} - \lambda e^{-a|n-p_2|} \\ (1+\lambda^2)e^{-a|n-p_2|} - \lambda(e^{-a|n-p_1|} + e^{-a|n-p_3|}) \\ \vdots \\ (1+\lambda^2)e^{-a|n-p_j|} - \lambda(e^{-a|n-p_{j-1}|} + e^{-a|n-p_{j+1}|}) \\ \vdots \\ (1+\lambda^2)e^{-a|n-p_{N_P-1}|} - \lambda(e^{-a|n-p_{N_P-2}|} + e^{-a|n-p_{N_P}|}) \\ e^{-a|n-p_{N_P}|} - \lambda e^{-a|n-p_{N_P-1}|} \end{bmatrix} \times \begin{bmatrix} 1 \\ 1-\lambda \\ \vdots \\ 1-\lambda \\ 1 \end{bmatrix}. \quad (35)$$

From this analytical expression, we are given the possibility to study the behavior of the Wiener filter when changing the parameters, e.g., a, b (or F_c) or the PT-RS spacing Δ . As this is not the target of the work presented here and given the limited size of the paper, we focus on the PT-RS selection only and we let this analysis to the interested reader.

III. COST FUNCTION DERIVATION

In this section, based on the formula of the Wiener filter coefficients (35), we construct a global cost function J stemming from the local cost functions J_n defined in (8) that explicitly includes the PT-RS spacing Δ (or the equivalent quantity λ). Similarly to the previous section, the mathematical details are available in [10]. Then, we show the behavior of the said function J as a function of a, b, F_c, Δ .

A. Cost function

We consider as the global cost function the sum of the local cost functions:

$$J = \sum_{n=1}^N J_n. \quad (36)$$

By developing the local cost function J_n from (8), we obtain:

$$J_n = 1 - 2\underline{w}_n^T \mathcal{R}\{\mathbb{E}[\alpha_n^* \hat{\alpha}_p]\} + \underline{w}_n^T \mathbb{E}[\hat{\alpha}_p \hat{\alpha}_p^\dagger] \underline{w}_n. \quad (37)$$

Then it comes that the global cost function is:

$$J = N - \sum_{n=1}^N \underline{w}_n^T \underline{\gamma}_n. \quad (38)$$

From (8) and (36), we observe that $J \geq 0$. In addition, by replacing \underline{w}_n with (9), we see that $\underline{w}_n^T \underline{\gamma}_n$ is a quadratic form, i.e., it is positive. Therefore, J is upper and lower bounded such that $0 \leq J \leq N$.

B. Derivation

We need to expand J as $J(\lambda)$, an explicit function of λ . To this end we need to compute the scalar product $\underline{w}_n^T \underline{\gamma}_n$ for all n . We expand $\underline{\gamma}_n$ as:

$$\underline{\gamma}_n = \frac{1}{1+c} \underline{\gamma}_n^{(0)} + \frac{c}{1+c} \underline{u}, \quad (39)$$

where \underline{u} is the full-one column vector of length N_p (see previous Section) and $\underline{\gamma}_{n,j}^{(0)} \stackrel{\text{def}}{=} e^{-a|n-p_j|}$.

For this part, we focus on computing $\underline{w}_n^T \underline{\gamma}_n^{(0)}$. As \underline{w}_n is a sum of two terms, we compute the product between the transpose of each of these terms and $\underline{\gamma}_n^{(0)}$. First of all, we can show that:

$$\begin{bmatrix} 1 \\ 1-\lambda \\ \vdots \\ 1-\lambda \\ 1 \end{bmatrix}^T \cdot \underline{\gamma}_n^{(0)} = \beta_n. \quad (40)$$

Secondly, we focus on the second term defining \underline{v}_n as:

$$\begin{aligned} v_{n,j} &= (1+\lambda^2)e^{-a|n-p_j|} - \lambda(e^{-a|n-p_{j-1}|} + e^{-a|n-p_{j+1}|}), \\ v_{n,1} &= e^{-a|n-p_1|} - \lambda e^{-a|n-p_2|}, \\ v_{n,N} &= e^{-a|n-p_{N_p}|} - \lambda e^{-a|n-p_{N_p-1}|}. \end{aligned} \quad (41)$$

It can be shown that:

$$\begin{aligned} \underline{v}_n^T \underline{\gamma}_n^{(0)} &= \sum_{j=1}^{N_p} \left(e^{-a|n-p_j|} \right)^2 + \sum_{j=2}^{N_p-1} \left(\lambda e^{-a|n-p_j|} \right)^2 \\ &\quad - 2\lambda \sum_{j=1}^{N_p-1} e^{-a|n-p_j|} e^{-a|n-p_{j+1}|}, \end{aligned} \quad (42)$$

which amounts to:

$$\begin{aligned} \underline{v}_n^T \underline{\gamma}_n^{(0)} &= \sum_{j=1}^{N_p-1} \left(e^{-a|n-p_j|} - \lambda e^{-a|n-p_{j+1}|} \right)^2 \\ &\quad + (1-\lambda^2)e^{-2a|n-p_{N_p}|}. \end{aligned} \quad (43)$$

Let's consider three cases to compute the sum: $n \leq p_1$, $p_1 < n < p_{N_p}$, $p_{N_p} \leq n$. For a given n , we introduce $K_p(n)$ the number of pilots before the index n :

$$K_p(n) \stackrel{\text{def}}{=} |\{j | p_j \leq n\}|. \quad (44)$$

Case 1: $n \leq p_1$

Here:

$$\underline{v}_n^T \underline{\gamma}_n^{(0)} = (1-\lambda^2)e^{-2a(p_1-n)} \left(1 - (1-\lambda)\lambda^{2(N_p-1)} \right) \quad (45)$$

Case 2: $p_1 < n < p_{N_p}$

Here:

$$\begin{aligned} \underline{v}_n^T \underline{\gamma}_n^{(0)} &= (1-\lambda^2)e^{-2a(p_1-n)} \lambda^{2K_p(n)} \\ &\quad + \lambda^2 \left(e^{-a(n-p_1)} \lambda^{-K_p(n)} - e^{-a(p_1-n)} \lambda^{K_p(n)} \right)^2. \end{aligned} \quad (46)$$

Case 3: $p_{N_p} \leq n$

Here:

$$\underline{v}_n^T \underline{\gamma}_n^{(0)} = (1-\lambda^2)e^{-2a(n-p_1)} \lambda^{2-2N_p}. \quad (47)$$

Now, we focus on computing $\underline{w}_n^T \underline{u}$. Actually, this product amounts to sum all the coordinates of $\underline{w}_n(\lambda)$. We can demonstrate that:

$$\underline{w}_n^T \underline{u} = \frac{1+\lambda-\beta_n}{(1+\lambda)(1+\lambda+\rho_\lambda)} \rho_\lambda + \frac{1}{1-\lambda^2} \sum_{j=1}^{N_p} v_{n,j}. \quad (48)$$

It appears that:

$$\begin{aligned} \frac{1}{1-\lambda^2} \sum_{j=1}^{N_p} v_{n,j} &= \frac{1}{1+\lambda} \left(\lambda(e^{-a|n-p_1|} + e^{-a|n-p_{N_p}|}) \right. \\ &\quad \left. + (1-\lambda) \sum_{j=1}^{N_p} e^{-a|n-p_j|} \right), \end{aligned} \quad (49)$$

where we recognize the component β_n such that:

$$\frac{1}{1-\lambda^2} \sum_{j=1}^{N_p} v_{n,j} = \frac{1}{1+\lambda} \beta_n, \quad (50)$$

therefore:

$$\underline{w}_n^T \underline{u} = \frac{1+\lambda-\beta_n}{(1+\lambda)(1+\lambda+\rho_\lambda)} \rho_\lambda + \frac{1}{1+\lambda} \beta_n. \quad (51)$$

These previous calculations allows us to obtain:

$$\begin{aligned} \underline{w}_n^T \underline{\gamma}_n &= c \frac{\beta_n(2(1+\lambda)-\beta_n) + \rho_\lambda(1+\lambda)}{(1+c)(1+\lambda)(1+\lambda+\rho_\lambda)} \\ &\quad + \frac{1}{(1+c)(1-\lambda^2)} \underline{v}_n^T \underline{\gamma}_n^{(0)}. \end{aligned} \quad (52)$$

This provides the expression of the cost function:

$$\begin{aligned} J(\lambda) &= N - \frac{c}{(1+c)(1+\lambda)(1+\lambda+\rho)} \\ &\quad \times \left(2(1+\lambda) \sum_{n=1}^N \beta_n - \sum_{n=1}^N \beta_n^2 + \rho(1+\lambda)N \right) \\ &\quad - \frac{1}{(1+c)(1-\lambda^2)} \sum_{n=1}^N \underline{v}_n^T \underline{\gamma}_n^{(0)}. \end{aligned} \quad (53)$$

To derive this calculation, we need to expand β_n and the sums of β_n and β_n^2 .

C. Derivation of β_n

We have to distinguish according to the value of n in comparison with the pilots position.

Case 1: $n < p_1$

Here, we can show that:

$$\beta_n = e^{-a(p_1-n)}(1 + \lambda). \quad (54)$$

Case 2: $p_1 \leq n < p_{N_P}$

Here, we can show that:

$$\beta_n = e^{-a(n-p_1)}\lambda^{1-K_P(n)} + e^{-a(p_1-n)}\lambda^{K_P(n)}. \quad (55)$$

Case 3: $p_{N_P} \leq n$

Here, we can show that:

$$\beta_n = e^{-a(n-p_1)}\lambda^{1-N_P}(1 + \lambda). \quad (56)$$

D. Derivation of $\sum_n \beta_n$

The sum over n is split into three sums as follows:

$$\begin{aligned} \sum_{n=1}^N \beta_n &= \sum_{n=1}^{p_1-1} \beta_n \\ &\quad + \sum_{n=p_1}^{p_{N_P}-1} \beta_n \\ &\quad + \sum_{n=p_{N_P}}^N \beta_n. \end{aligned} \quad (57)$$

It can be shown that:

$$\sum_{n=1}^{p_1-1} \beta_n = (1 + \lambda) \frac{e^{-a(p_1-1)} - 1}{1 - e^a}, \quad (58)$$

$$\sum_{n=p_{N_P}}^N \beta_n = (1 + \lambda) \frac{1 - \lambda^{1-N_P} e^{-a(N+1-p_1)}}{1 - e^a}. \quad (59)$$

To compute the sum for $p_1 < n < p_{N_P}$, we consider a first split according to the expression of β_n :

$$\begin{aligned} \sum_{n=p_1}^{p_{N_P}-1} \beta_n &= \lambda e^{ap_1} \sum_{n=p_1}^{p_{N_P}-1} e^{-an} \lambda^{-K_P(n)} \\ &\quad + e^{-ap_1} \sum_{n=p_1}^{p_{N_P}-1} e^{an} \lambda^{K_P(n)}, \end{aligned} \quad (60)$$

then, we split each of both sums into sub-sums where each of them goes from one pilot position p_j to the next one $p_{j+1} - 1$ such that:

$$\sum_{n=p_1}^{p_{N_P}-1} e^{-an} \lambda^{-K_P(n)} = \sum_{j=1}^{N_P-1} \sum_{n=p_j}^{p_{j+1}-1} e^{-an} \lambda^{-K_P(n)}, \quad (61)$$

$$\sum_{n=p_1}^{p_{N_P}-1} e^{an} \lambda^{K_P(n)} = \sum_{j=1}^{N_P-1} \sum_{n=p_j}^{p_{j+1}-1} e^{an} \lambda^{K_P(n)}. \quad (62)$$

The rationale behind is that for any $p_j \leq n < p_{j+1}$ we observe that $K_P(n) = j$. Therefore:

$$\sum_{n=p_1}^{p_{N_P}-1} e^{-an} \lambda^{-K_P(n)} = \sum_{j=1}^{N_P-1} \lambda^{-j} \sum_{n=p_j}^{p_{j+1}-1} e^{-an}, \quad (63)$$

$$\sum_{n=p_1}^{p_{N_P}-1} e^{an} \lambda^{K_P(n)} = \sum_{j=1}^{N_P-1} \lambda^j \sum_{n=p_j}^{p_{j+1}-1} e^{an}. \quad (64)$$

Now it comes that:

$$\sum_{n=p_1}^{p_{N_P}-1} e^{-an} \lambda^{-K_P(n)} = e^{-ap_1} (N_P - 1) \frac{1 - \lambda}{\lambda(1 - e^{-a})}, \quad (65)$$

$$\sum_{n=p_1}^{p_{N_P}-1} e^{an} \lambda^{K_P(n)} = e^{ap_1} (N_P - 1) \frac{\lambda - 1}{1 - e^a}. \quad (66)$$

This provides then the middle sum of β_n :

$$\sum_{n=p_1}^{p_{N_P}-1} \beta_n = (N_P - 1)(1 - \lambda) \left(\frac{1}{1 - e^{-a}} - \frac{1}{1 - e^a} \right). \quad (67)$$

Therefore, the total sum is:

$$\begin{aligned} \sum_{n=1}^N \beta_n &= \frac{1 + \lambda}{1 - e^a} \left(e^{-a(p_1-1)} - 1 \right) \\ &\quad + (N_P - 1)(1 - \lambda) \left(\frac{1}{1 - e^{-a}} - \frac{1}{1 - e^a} \right) \\ &\quad + \frac{1 + \lambda}{1 - e^a} \left(1 - \lambda^{1-N_P} e^{-a(N+1-p_1)} \right). \end{aligned} \quad (68)$$

This can also be written as:

$$\begin{aligned} \sum_{n=1}^N \beta_n &= \left(\lambda(N_P - 2) - N_P \right) \frac{1 + e^a}{1 - e^a} \\ &\quad + \frac{1 + \lambda}{1 - e^a} \left(e^{-a(p_1-1)} + e^{-a(N-p_1)} \lambda^{1-N_P} \right) \end{aligned} \quad (69)$$

E. Derivation of $\sum_n \beta_n^2$

Similarly, the sum over n is split into three sums as follows:

$$\begin{aligned} \sum_{n=1}^N \beta_n^2 &= \sum_{n=1}^{p_1-1} \beta_n^2 \\ &\quad + \sum_{n=p_1}^{p_{N_P}-1} \beta_n^2 \\ &\quad + \sum_{n=p_{N_P}}^N \beta_n^2. \end{aligned} \quad (70)$$

It can be shown that:

$$\sum_{n=1}^{p_1-1} \beta_n^2 = (1 + \lambda)^2 \frac{e^{-2a(p_1-1)} - 1}{1 - e^{2a}}, \quad (71)$$

$$\sum_{n=p_{N_P}}^N \beta_n^2 = (1 + \lambda)^2 \frac{1 - \lambda^{2(1-N_P)} e^{-2a(N+1-p_1)}}{1 - e^{-2a}}. \quad (72)$$

In the same manner as previously, we can show that:

$$\sum_{n=p_1}^{p_{N_P}-1} \beta_n^2 = 2\lambda\Delta(N_P - 1) + (1 - \lambda^2)(N_P - 1) \frac{e^{2a} + 1}{e^{2a} - 1}. \quad (73)$$

We can then merge these three sums together to obtain:

$$\begin{aligned} \sum_{n=1}^N \beta_n^2 &= (1 + \lambda) \left(\lambda(N_P - 2) - N_P \right) \frac{1 + e^{2a}}{1 - e^{2a}} \\ &+ \frac{(1 + \lambda)^2}{1 - e^{2a}} \left(e^{-2a(p_1-1)} + \lambda^{2(1-N_P)} e^{-2a(N-p_1)} \right) \\ &+ 2\lambda\Delta(N_P - 1) \end{aligned} \quad (74)$$

F. Derivation of $J_\beta(\lambda)$

We define the quantity:

$$J_\beta(\lambda) \stackrel{\text{def}}{=} 2(1 + \lambda) \sum_{n=1}^N \beta_n - \sum_{n=1}^N \beta_n^2, \quad (75)$$

which is part of the total cost function $J(\lambda)$. We can show that:

$$\begin{aligned} J_\beta(\lambda) &= (1 + \lambda) \left(\lambda(N_P - 2) - N_P \right) \frac{(1 - e^a)^2 + 6e^a}{1 - e^{2a}} \\ &+ \frac{(1 + \lambda)^2}{1 - e^a} \left(2e^{-a(p_1-1)} + 2e^{-a(N-p_1)} \lambda^{1-N_P} \right. \\ &- \frac{e^{-2a(p_1-1)}}{1 + e^a} - \frac{e^{-2a(N-p_1)} \lambda^{2(1-N_P)}}{1 + e^a} \Big) \\ &- 2\lambda\Delta(N_P - 1) \end{aligned} \quad (76)$$

G. Derivation of $\sum_n \underline{v}_n^T \underline{\gamma}_n^{(0)}$

Similarly to the sum of β_n we split the sum into three sums such that:

$$\begin{aligned} \sum_{n=1}^N \underline{v}_n^T \underline{\gamma}_n^{(0)} &= \sum_{n=1}^{p_1-1} \underline{v}_n^T \underline{\gamma}_n^{(0)} \\ &+ \sum_{n=p_1}^{p_{N_P}-1} \underline{v}_n^T \underline{\gamma}_n^{(0)} \\ &+ \sum_{n=p_{N_P}}^N \underline{v}_n^T \underline{\gamma}_n^{(0)}. \end{aligned} \quad (77)$$

We can show that:

$$\begin{aligned} \sum_{n=1}^{p_1-1} \underline{v}_n^T \underline{\gamma}_n^{(0)} &= (1 - \lambda^2) \left(1 - (1 - \lambda) \lambda^{2(N_P-1)} \right) \\ &\times \frac{e^{-2a(p_1-1)} - 1}{1 - e^{2a}}, \end{aligned} \quad (78)$$

and that:

$$\sum_{n=p_{N_P}}^N \underline{v}_n^T \underline{\gamma}_n^{(0)} = (1 - \lambda^2) \frac{1 - \lambda^{2(1-N_P)} e^{-2a(N+1-p_1)}}{1 - e^{-2a}}. \quad (79)$$

For the sum on middle values of n , we use the same method as for the sum on middle values of β_n , i.e.:

$$\sum_{n=p_1}^{p_{N_P}-1} \underline{v}_n^T \underline{\gamma}_n^{(0)} = \sum_{j=1}^{N_P-1} \sum_{n=p_j}^{p_{j+1}-1} \underline{v}_n^T \underline{\gamma}_n^{(0)}, \quad (80)$$

which gives:

$$\begin{aligned} \sum_{n=p_1}^{p_{N_P}-1} \underline{v}_n^T \underline{\gamma}_n^{(0)} &= (1 - \lambda^2) e^{-2ap_1} \sum_{j=1}^{N_P-1} \sum_{n=p_j}^{p_{j+1}-1} \lambda^{2K_P(n)} e^{2an} \\ &+ \lambda^2 \sum_{j=1}^{N_P-1} \sum_{n=p_j}^{p_{j+1}-1} \left(e^{-a(n-p_1)} \lambda^{-K_P(n)} \right. \\ &- e^{-a(p_1-n)} \lambda^{K_P(n)} \Big)^2. \end{aligned} \quad (81)$$

We can then show that:

$$\sum_{n=p_1}^{p_{N_P}-1} \underline{v}_n^T \underline{\gamma}_n^{(0)} = (1 - \lambda^2)(N_P - 1) \frac{e^{2a} + 1}{e^{2a} - 1} - 2\lambda^2\Delta(N_P - 1) \quad (82)$$

Finally, the total sum can be demonstrated to equal:

$$\begin{aligned} \sum_{n=1}^N \underline{v}_n^T \underline{\gamma}_n^{(0)} &= \frac{1 - \lambda^2}{1 - e^{2a}} \left(e^{-2a(p_1-1)} - N_P(e^{2a} + 1) \right. \\ &+ \lambda^{2(1-N_P)} e^{-2a(N-p_1)} \\ &- (1 - \lambda) \lambda^{2(N_P-1)} (e^{-2a(p_1-1)} - 1) \Big) \\ &- 2\lambda^2\Delta(N_P - 1) \end{aligned} \quad (83)$$

At this stage, from the previous calculations, we are provided a one-dimensional closed form of the cost function $J(\lambda)$:

$$\begin{aligned} J(\lambda) &= N - \frac{1}{1 + c} \left[\frac{c}{1 + \lambda + \rho_\lambda} \left(\rho_\lambda \left(N - \frac{(1 - e^a)^2 + 6e^a}{c(1 - e^{2a})} \right) \right. \right. \\ &+ \frac{1 + \lambda}{1 - e^a} \left(2e^{-a(p_1-1)} + 2e^{-a(N-p_1)} \lambda^{1-N_P} \right. \\ &- \frac{e^{-2a(p_1-1)} + e^{-2a(N-p_1)} \lambda^{2(1-N_P)}}{1 + e^a} \Big) \Big) \\ &+ \frac{1}{1 - e^{2a}} \left(e^{-2a(p_1-1)} - N_P(e^{2a} + 1) + \lambda^{2(1-N_P)} e^{-2a(N-p_1)} \right. \\ &- (1 - \lambda) \lambda^{2(N_P-1)} (e^{-2a(p_1-1)} - 1) \Big) \\ &- \frac{\lambda}{1 + \lambda} 2\Delta(N_P - 1) \left(\frac{c}{1 + \lambda + \rho_\lambda} + \frac{\lambda}{1 - \lambda} \right) \Big] \end{aligned} \quad (84)$$

By identification, it can be shown that $J(\lambda)$ has a quasi-polynomial form such that:

$$J(\lambda) = N - \frac{1}{1+c} \frac{J^{(N)}(\lambda)}{J^{(D)}(\lambda)}. \quad (85)$$

$J^{(N)}(\lambda)$ is defined with the monomials $\{j_k^{(N)}\}_k$ from Table I such that:

$$\begin{aligned} J^{(N)}(\lambda) = & j_{2N_P+2}^{(N)} \lambda^{2N_P+2} + j_{2N_P+1}^{(N)} \lambda^{2N_P+1} \\ & + j_{2N_P}^{(N)} \lambda^{2N_P} + j_{2N_P-1}^{(N)} \lambda^{2N_P-1} \\ & + j_{2N_P-2}^{(N)} \lambda^{2N_P-2} \\ & + j_3^{(N)} \lambda^3 + j_2^{(N)} \lambda^2 + j_1^{(N)} \lambda + j_0^{(N)} \\ & + j_{4-N_P}^{(N)} \lambda^{4-N_P} + j_{3-N_P}^{(N)} \lambda^{3-N_P} \\ & + j_{2-N_P}^{(N)} \lambda^{2-N_P} + j_{1-N_P}^{(N)} \lambda^{1-N_P} \\ & + j_{5-2N_P}^{(N)} \lambda^{5-2N_P} + j_{4-2N_P}^{(N)} \lambda^{4-2N_P} \\ & + j_{3-2N_P}^{(N)} \lambda^{3-2N_P} + j_{2-2N_P}^{(N)} \lambda^{2-2N_P} \\ & + \frac{\log \lambda}{a} \left(j j_3^{(N)} \lambda^3 + j j_2^{(N)} \lambda^2 + j j_1^{(N)} \lambda \right), \end{aligned} \quad (86)$$

and:

$$\begin{aligned} j j_3^{(N)} &= 2(1 - N_P)(1 + c(2 - N_P)), \\ j j_2^{(N)} &= 2(1 - N_P)(1 + c(N_P - 1)), \\ j j_1^{(N)} &= 2(1 - N_P)c. \end{aligned} \quad (87)$$

$J^{(D)}(\lambda)$ is defined with the monomials $\{j_k^{(D)}\}_k$ such that:

$$J^{(D)}(\lambda) = j_3^{(D)} \lambda^3 + j_2^{(D)} \lambda^2 + j_1^{(D)} \lambda + j_0^{(D)}, \quad (88)$$

and:

$$\begin{aligned} j_3^{(D)} &= c(N_P - 2) - 1, \\ j_2^{(D)} &= -(1 + cN_P), \\ j_1^{(D)} &= -j_3^{(D)}, \\ j_0^{(D)} &= -j_2^{(D)}. \end{aligned} \quad (89)$$

H. Influence of a, b and F_c

Using the values of a and b from Fig. 2, we show the behavior of J against a and b in Fig. 3 assuming a PT-RS spacing of $\Delta = 50$ in a signal of length $N = 4096$.

J exhibits a linear behavior with a and b which is convenient to predict its values. Similarly to the autocorrelation, see I-B, J varies more with b than with a . As a decrease in b corresponds to an increase in F_c that means an increase in the phase noise intensity, then, a decrease in b involves a degradation of the Wiener filter performance while keeping the same values for Δ, N . This explains why J is a decreasing function of b .

Given that a value of the couple (a, b) corresponds to a single value of F_c , we can show the evolution of J with F_c for various values of the PT-RS spacing Δ , see Fig. 4. This figure shows the maximum carrier frequency for a PT-RS spacing: when setting a maximum value for J , i.e. a maximum cost, we are indeed able to find the maximum carrier frequency

k	$j_k^{(N)}$
$2N_P + 2$	$\frac{e^{-2a(p_1-1)} - 1}{e^{2a} - 1} (1 + c(2 - N_P))$
$2N_P + 1$	$2c \frac{e^{-2a(p_1-1)} - 1}{1 - e^{2a}} (1 - N_P)$
$2N_P$	$2(1 + c) \frac{e^{-2a(p_1-1)} - 1}{1 - e^{2a}}$
$2N_P - 1$	$-j_{2N_P+1}^{(N)}$
$2N_P - 2$	$\frac{e^{-2a(p_1-1)} - 1}{e^{2a} - 1} (1 + cN_P)$
3	$\left((1 + c(2 - N_P)) (N_P(e^{2a} + 1) - e^{-2a(p_1-1)}) \right. \\ \left. + c(N_P - 2) (cN(1 - e^{2a}) - (1 - e^a)^2 - 6e^a) \right. \\ \left. - 2ce^{-a(p_1-1)}(e^a + 1) + ce^{-2a(p_1-1)} \right) / (1 - e^{2a})$
2	$c^2 N_P \left(\frac{6e^a + (1 - e^a)^2}{c(1 - e^{2a})} - N \right) \\ + \frac{e}{1 - e^a} \left(\frac{e^{-2a(p_1-1)}}{e^a + 1} - 2e^{-a(p_1-1)} \right) \\ + \frac{1 + cN_P}{1 - e^{2a}} (N_P(e^{2a} + 1) - e^{-2a(p_1-1)})$
1	$-j_3^{(N)}$
0	$-j_2^{(N)}$
$4 - N_P$	$2c \frac{e^{-a(N-P_1)}}{e^a - 1}$
$3 - N_P$	$j_{4-N_P}^{(N)}$
$2 - N_P$	$-j_{4-N_P}^{(N)}$
$1 - N_P$	$-j_{4-N_P}^{(N)}$
$5 - 2N_P$	$\frac{e^{-2a(N-P_1)}}{e^{2a} - 1} (1 + c(1 - N_P))$
$4 - 2N_P$	$\frac{e^{-2a(N-P_1)}}{e^{2a} - 1} (1 + c(N_P - 1))$
$3 - 2N_P$	$-j_{5-2N_P}^{(N)}$
$2 - 2N_P$	$-j_{4-2N_P}^{(N)}$

TABLE I
MONOMIALS OF THE NUMERATOR.

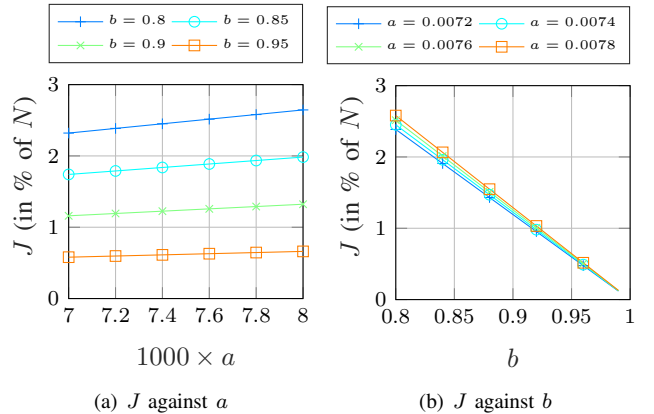


Fig. 3. Global cost function J against a and b .

value for which a given spacing leads to a Wiener filter with acceptable performance with respect to the said cost. As an example, when requiring that $J \leq 2\%$, the PT-RS spacing $\Delta = 100$ becomes irrelevant when $F_c \geq 200\text{GHz}$.

I. Influence of Δ

We observe in Fig. 5 the evolution of J as a function of the PT-RS spacing Δ for various values of F_c . J shows an affine

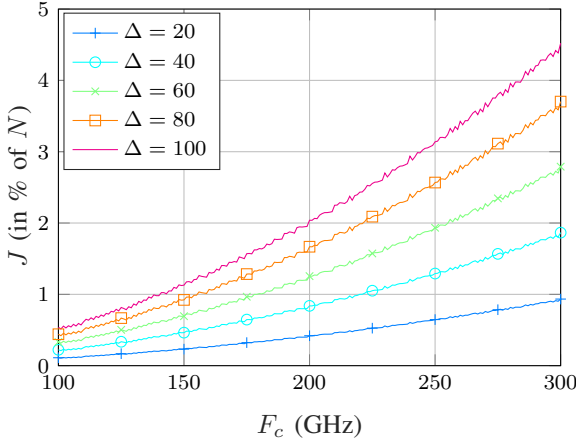


Fig. 4. Global cost function against the carrier frequency F_c for various values of Δ .

behavior such that we can approximate it as follows:

$$J(\Delta) \approx \omega \Delta + \eta. \quad (90)$$

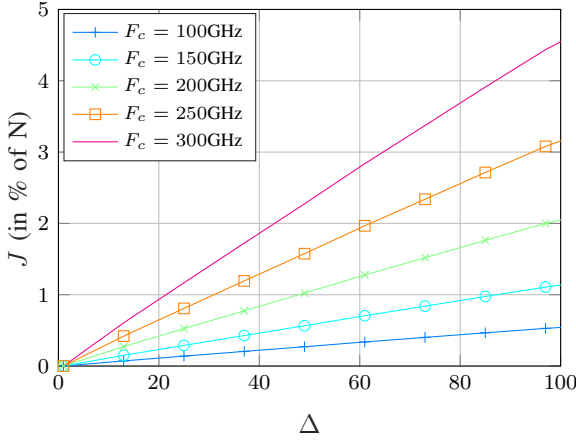


Fig. 5. Global cost function against the PT-RS spacing for various values of the carrier frequency F_c .

The slope ω and the y-intersect η can be deduced from (85). However, at this stage, the affine reduction of (85) is not tractable. Therefore, we obtain (90) through a linear interpolation of J , see in Fig. 6 the evolution of ω and η with the carrier frequency. The best model with respect to the mean square error is:

$$\begin{aligned} \omega(F_c) &\approx 5.03 \cdot 10^{-25} F_c^2 \text{ (in \% of N)}, \\ \eta(F_c) &\approx 2.17 \cdot 10^{-25} F_c^2 \text{ (in \% of N)}. \end{aligned} \quad (91)$$

IV. PT-RS EXTRACTION

In this section, we show how to extract λ^* (or Δ^*) that leads to the best performance of the Wiener filter in terms of the associated cost function defined in the previous section. This section exposes how to consider a performance constraint as

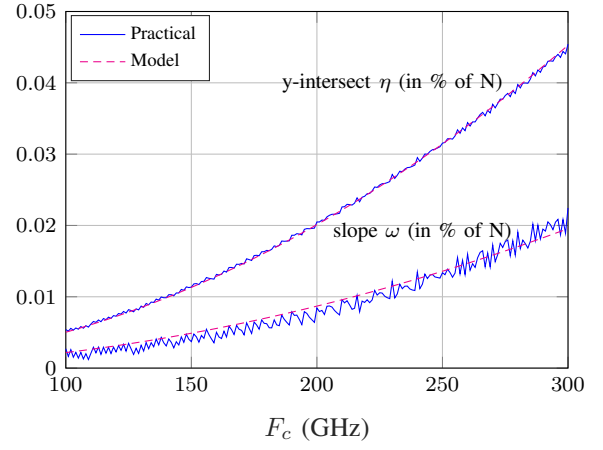


Fig. 6. Slope and y-intersect of the linear approximation of $J(\Delta)$ against F_c and an approximate model.

well as an overhead constraint accompanied with an application example.

A. Constraints

To ensure a minimum data rate that corresponds to a reasonable PT-RS overhead, we consider a minimum PT-RS spacing Δ_0 . As J is an increasing function of Δ , setting $\Delta = \Delta_0$ surely performs the best. Yet, the Wiener filter may have acceptable performance even when enlarging the spacing up to a maximum value Δ_{PF} . In other words, we assert that while $\Delta_0 \leq \Delta \leq \Delta_{PF}$, the Wiener filter well performs with Δ . In the next paragraph, we show how to determine the value Δ_{PF} based on the result from the previous section.

As the PT-RS distribution is uniform, we can assume that the number of PT-RS for a given spacing Δ is $N_P = \lceil \frac{N}{\Delta} \rceil$. The PT-RS overhead being the ratio between N_P and N , we deduce that it is closed to $\frac{1}{\Delta}$.

B. Example of use

We consider here that an experimenter requires the communication chain to perform at 300GHz such that the Wiener filter performs such that the cost J remains below $MaxCost = 2.5\%$. Moreover, the experimenter requires a minimum throughput such that the PT-RS spacing should not decrease below $\Delta_0 = 20$ assuming signals of length $N = 4096$. By choosing $\Delta = \Delta_0$ we obtain a PT-RS overhead of 5%. From the previous approximations, we can set:

$$\omega(F_c = 300\text{GHz}) = 0.0453 \text{ (in \% of N)}, \quad (92)$$

$$\eta(F_c = 300\text{GHz}) = 0.0195 \text{ (in \% of N)}. \quad (93)$$

We observe that $J(\Delta_0) \approx 0.9248\%$ which is below $MaxCost$. Therefore, we can propose a PT-RS spacing larger than Δ_0 to fulfill the cost constraint while ensuring an acceptable expected spectral efficiency. By inverting the affine approximation, we obtain the maximum spacing Δ_{PF} :

$$\Delta_{PF} = \left\lceil \frac{MaxCost - \eta(F_c = 300\text{GHz})}{\omega(F_c = 300\text{GHz})} \right\rceil = 54. \quad (94)$$

With this spacing, the resulting PT-RS overhead is reduced to 1.85% which leaves a significant space for the data symbols. This example is shown in Fig. 7.

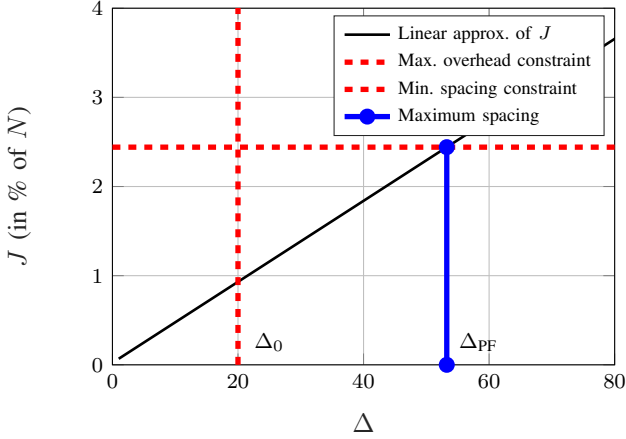


Fig. 7. Example of the optimal pilot pattern extraction at $F_c = 300\text{GHz}$.

CONCLUSION

In this paper, we presented a method to obtain the spacing between PT-RS positions that allows acceptable performance of the Wiener filter, used to track the phase noise, while ensuring a sufficiently small pilot overhead. We considered an analytical derivation of the cost function whose behavior is monotonic, leading to a straightforward selection of the spacing given the said constraints on the overhead and the performance. The derivation relied on an exponential approximation of the autocorrelation of the 3GPP phase noise model.

[8] J.-C. Sibel, "Tracking the phase noise in sub-thz bands," in *2022 IEEE Wireless Communications and Networking Conference (WCNC)*, 2022.

In future works, one could target an enhancement of the said approximation to better fit with the model for very high values of the carrier frequencies toward THz.

REFERENCES

- [1] *TS38.101-2 Technical Specification Group Radio Access Network; NR; User Equipment (UE) radio transmission and reception; Part 2: Range 2 Standalone (Release 18); Sec. 5.2*, 3rd Generation Partnership Project (3GPP), December 2022, v18.0.0.
- [2] A. Shafie, N. Yang, C. Han, J. M. Jornet, M. Juntti, and T. Kurner, "Terahertz Communications for 6G and Beyond Wireless Networks: Challenges, Key Advancements, and Opportunities," <https://arxiv.org/pdf/2207.11021>, in arXiv, 2022.
- [3] *TS38.211 Technical Specification Group Radio Access Network; NR; Physical channels and modulation (Release 17); Sec. 6.4.1.2*, 3rd Generation Partnership Project (3GPP), December 2022, v17.4.0.
- [4] ShareTechnote, "5G/NR - PHY Candidate, DFT-s-OFDM," https://www.sharetechnote.com/html/5G/5G_Phy_Candidate_DFTsOFDM.html.
- [5] 3rd Generation Partnership Project (3GPP), "R1-1712032 Final Report of 3GPP TSG RAN WG1 AH NR2 v1.0.0. Sec. 5.1.2.4.4," in *3GPP TSG RAN WG1 Meeting 90, Prague, Czech Rep.*, August 2017.
- [6] A. V. Oppenheim and G. C. Verghese, *Introduction to Communication, Control and Signal Processing. Spring 2010. Chapter 11*. Massachusetts Institute of Technology, 2010.
- [7] *TR38.808 Technical Specification Group Radio Access Network; Study on supporting NR from 52.6 GHz to 71 GHz (Release 17); Sec. 4.2.3.1*, 3rd Generation Partnership Project (3GPP), March 2021, v17.0.0.
- [9] S. Bicaïs and J.-B. Dore, "Phase noise model selection for sub-thz communications," in *2019 IEEE Global Communications Conference (GLOBECOM)*, 2019.
- [10] J.-C. Sibel, V. Corlay, and A. Bechihi, "Optimized pilot distribution to track the phase noise in DFT-s-OFDM for sub-THz systems. Appendix for calculations," in arXiv, 2023.
- [11] Mathematics Stack Exchange, achille hui (<https://math.stackexchange.com/users/59379/achille-hui>), "Closed form inverse for the matrix $\exp(-|m - n|)$," <https://math.stackexchange.com/q/2274850>.